Phys. Status Solidi A **209,** No. 8, 1461–1466 (2012) / **DOI** 10.1002/pssa.201228065

physica status solidi a
www.pss-a.com
applications and materials science

Influence of pulsed laser annealing on the optical properties of ZnO nanorods

T. N. Lin[1], C. P. Huang[1], G. W. Shu[1], J. L. Shen[*,1], C. S. Hsiao[2], and S. Y. Chen[2]

[1] Department of Physics and Center for Nanotechnology at CYCU, Chung Yuan Christian University, Chung-Li, Taiwan
[2] Department of Materials Science and Engineering, National Chiao Tung University, Hsin-Chu, Taiwan

Received 30 January 2012, revised 13 April 2012, accepted 13 April 2012
Published online 17 May 2012

Keywords nanorods, pulsed laser annealing, rapid thermal annealing, ZnO

[*] Corresponding author: e-mail jlshen@cycu.edu.tw, Phone: 886-3-2653227, Fax: 886-3-2653299

The effect of pulsed laser annealing (PLA) on the photoluminescence (PL) properties of ZnO nanorods was investigated. As the fluence of pulsed laser increases, the UV PL in ZnO nanorods shows a general increasing trend, except at a range of fluences from 10 to 70 mJ/cm^2. It is found that the treatment with the PLA at the fluence of 70 mJ/cm^2 leads to a larger improvement of crystalline properties than that with rapid thermal annealing (RTA). The relationship between PL intensity and fluence of pulsed lasers can be well explained by a combination of the deterioration in surface crystallinity and the increased donor densities after PLA.

1 Introduction ZnO is a wide direct bandgap semiconductor with considerable interest for optoelectronic devices. The room-temperature binding energy of free electrons in ZnO is 60 meV, which makes the electrons stable at room temperature [1, 2]. Hence, ZnO is a promising material for devices such as the ultraviolet light-emitting diodes, laser diodes, gas sensors, and probes of atomic force microscopy [3–7]. Among the ZnO materials, one-dimensional ZnO nanostructures such as nanowires and nanotubes exhibit novel and device applicable physical properties, which can be used in a wide variety of applications [8–10]. The one-dimensional ZnO nanorods are interesting materials since they have excellent optical properties owing to their high surface-to-volume ratio.

It is well known that postgrowth annealing is an effective technique to eliminate the nonradiative defects and/or improve the quality of semiconductors. The effects of postgrowth annealing on the optical and electrical properties of ZnO nanorods have been studied [12–16]. The ratio of UV to visible luminescence was greatly changed after annealing processes [11–15]. The PL change after annealing in ZnO has been attributed to the enhanced stoichiometric Zn–O bonding [12], reduction in the nonradiative related defects [13], and removal of functional groups (surface oxygen species) [14, 16]. Postgrowth annealing can be carried out by various techniques, such as thermal annealing, rapid thermal annealing (RTA), and pulsed laser annealing (PLA). Among these techniques, PLA is a special one to anneal the target material by choosing a wavelength that is strongly absorbed in that material, while being weakly absorbed in the environment [11]. PLA is thus expected to be a convenient method to allow a local annealing in materials or devices. Recently, there is one report that studied the effects of PLA on ZnO nanorods [11]. Nadarajah and Könenkamp [11] have found that the excitonic luminescence in ZnO nanorods can be increased by a factor of 8 by changing the pulsed laser energy and illumination time. However, the mechanisms that caused the enhancement of PL after PLA have not been understood yet. The effects of the illumination of a pulsed laser on the surface morphology and/or the temperature of ZnO nanorods is still unknown.

In this work, we perform the PLA in ZnO nanorods on Si substrates. On increasing the incident laser power (fluence) in PLA, the UV PL intensity increases. RTA was also performed to estimate the surface temperature of ZnO nanorods after PLA. The possible origin for the enhancement of the UV PL in ZnO nanorods is discussed.

2 Experiments The ZnO nanorods investigated were grown on the Si substrate. A ZnO-buffered layer (with a thickness of around 100 nm) was deposited on the substrate by radio-frequency (rf) magnetron sputtering using 99.99% ZnO as the target. Then, the ZnO-coated substrates were placed in an equimolar (0.01 M) aqueous solution of $Zn(NO_3)_2 \cdot 6H_2O$ and hexamethylenetetramine (HMT) at

75 °C for 10 h. Subsequently, the substrates were removed from the aqueous solutions, rinsed in distilled water, and dried overnight at room temperature. The length and diameter of the grown ZnO nanorods is about 1 μm and 100 nm, respectively. Figure 1 shows the schematic representation of the ZnO nanorods grown on Si substrates. The PLA was performed in an uncovered cryostat in ambient air at room temperature. The ZnO nanorods were irradiated for 10 s with a pulsed laser with a wavelength of 266 nm and a pulse frequency 10 Hz. The laser pulse energy is 10–70 mJ/cm^2, resulting from the Nd-YAG fourth-harmonic laser. The laser beam was focused onto the target with an incident angle of 45 and the fluence on the ZnO nanorods was changed from 10 to 70 mJ/cm^2. The ZnO nanorods were also treated with RTA using tungsten-halogen lamps at temperatures from 200 to 900 °C and in a flowing nitrogen gas ambient. During the RTA process, temperature was first ramped up from room temperature to the selected temperature with a ramp rate of 30 °C/s, maintained at that temperature with an annealing time of 5 s and ramped down to room temperature. The PL measurements were obtained using a focused HeCd laser operating with a wavelength of 325 nm and with a power of 1 mW as the excitation source. The sample was mounted in a close–cycle helium cryostat and the sample temperature was controlled between 15 and 300 K. The laser beam for PL was focused on the sample with an incident angle of 45°. In this geometry, most of the laser was absorbed by the 1-μm long ZnO nanorods, not the 100-nm-thick ZnO buffer layer since the absorption length of the incident photon for ZnO is ~0.2 μm at the wavelength of 325 nm [17]. In other words, the PL spectroscopy is mostly related to the ZnO nanorods, not the ZnO buffer layer. The collected luminescence was dispersed by a 0.75-m spectrometer and detected with the photomultiplier tube.

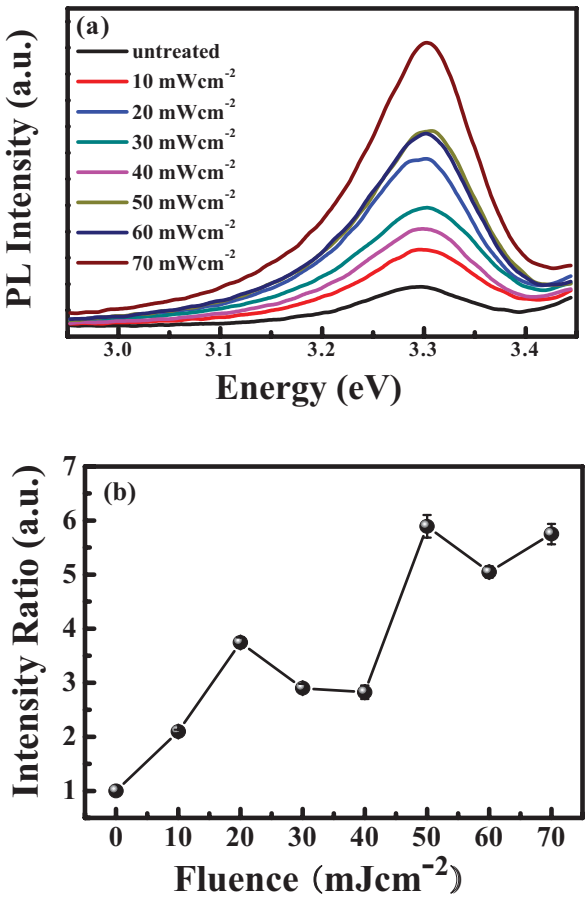

Figure 2 (online color at: www.pss-a.com) (a) PL spectra of the ZnO nanorods before and after PLA at different fluence. (b) The PL intensity ratio of the PLA-treated to untreated ZnO nanorods as a function of the irradiation energy density. The line is a guide for the eye.

3 Results and discussion Figure 2a shows the PL spectra of the as-grown and pulse-laser-irradiated ZnO nanorods. The PL data display a clear peak in UV spectral range. After the sample is annealed under the pulsed laser, the peak position of PL shows no obvious change, while a remarkably strong enhancement in PL intensity is found. An increase of the UV PL by a factor of 6 is observed after 70 mJ/cm^2 of exposure. The intensity of UV PL as a function of fluence is plotted in Fig. 2b. The PL intensity increases significantly at a range of fluences from 10 to 20 mJ/cm^2, then decreases over a range of fluencies 20–40 mJ/cm^2. After a fluence of 40 mJ/cm^2, the PL intensity keeps roughly constant. For the ZnO bulk materials PLA has been performed by the KrF excimer laser, inducing a change of intensity in UV emission [18, 19]. However, the effect of the PLA influence on the UV emission in ZnO nanorods has not been reported before.

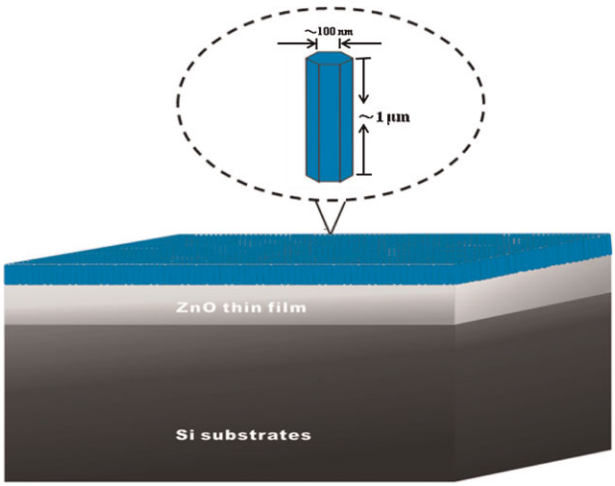

Figure 1 (online color at: www.pss-a.com) Schematic representation of the ZnO nanorod arrays grown on Si substrates. The corresponding SEM image is shown in Fig. 6a.

Figure 3a shows the PL spectra of the ZnO nanorods before and after RTA at room temperature. It is found that the PL intensity increases as the RTA temperature (T_{RTA}) is increased from 200 to 500 °C. As T_{RTA} increases from 500 to 700 °C, a decrease in the PL intensity is found. At $T_{RTA} = 800$ °C, the PL intensity has a maximum value, which increases by about a factor of 2 compared with that of

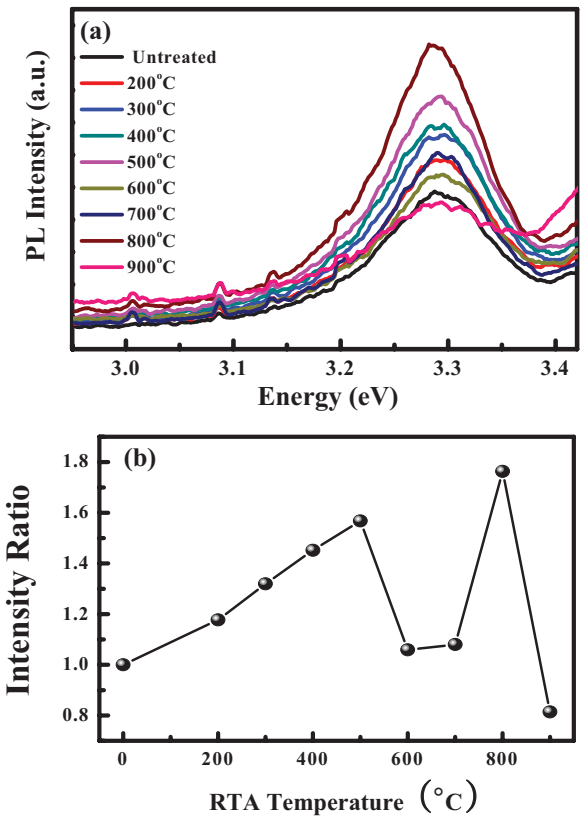

Figure 3 (online color at: www.pss-a.com) (a) PL spectra of the ZnO nanorods before and after RTA at different T_{RTA}. (b) The PL intensity ratio of the RTA-treated to untreated ZnO nanorods as a function of the RTA temperature. The line is a guide for the eye.

the untreated sample. Figure 3b shows the PL intensity as a function of T_{RTA}. We notice that the trend of the PL intensity versus fluence in PLA (Fig. 2b) has similarity to that versus T_{RTA} in RTA (Fig. 3b). In the beginning, the PL intensity increases with fluence (T_{RTA}) for PLA (RTA). The PL intensity then decreases at a range of fluences (T_{RTA}) from 20 to 40 mJ/cm^2 (from $T_{RTA} = 500$ to 700 °C) for PLA (RTA). Finally, the PL intensity increases again for a fluence of 50 mJ/cm^2 ($T_{RTA} = 800$ °C) for PLA (RTA). With this relation, we can estimate the surface temperature of ZnO nanorods after the effect of PLA. The surface temperature of ZnO nanorods after the illumination of 20, 40, and 50 mJ/cm^2 roughly corresponds to ~500, 700, and 800 °C, respectively. Therefore, by measuring PLA and RTA simultaneously, it is possible to determine the surface temperature of ZnO nanorods after the illumination of pulsed lasers.

It is interesting to investigate which annealing technique can be more effective for improving the PL properties in ZnO nanorods since PLA and RTA are commonly employed to improve sample quality. Figure 4 shows the 9 K PL of ZnO nanorods with PLA at a fluence of 70 mJ/cm^2 and with RTA at $T_{RTA} = 800$ °C. At low temperatures, PL data display two clear peaks at energies of ~3.375 and 2.85 eV. A lot of peaks have previously been observed by a number of authors in the

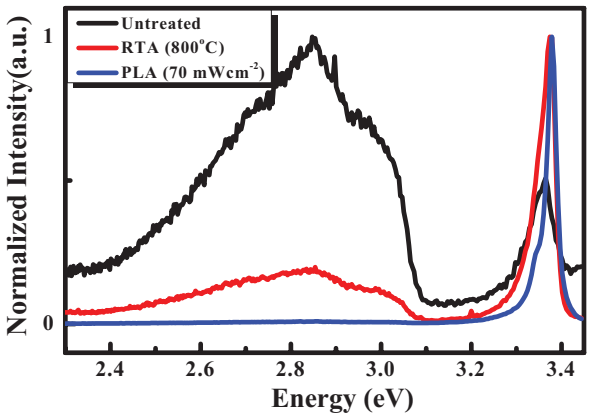

Figure 4 (online color at: www.pss-a.com) The 9 K PL spectra of the ZnO nanorods before and after annealing. The black, red, and blue lines indicate the PL spectra of the untreated, RTA at 800 °C, and PLA at the fluence of 70 mJ/cm^2, respectively.

studies of ZnO samples. The high-energy peak at ~3.375 eV is attributed to the bound exciton emission [20]. On the other hand, the broad visible peak at 2.85 eV may be due to the defect PL. Defects are usually generated in the ZnO nanorods at a relatively low growth temperature by an aqueous method. The relative integrated PL intensity ratio between the UV emission and defect emission is normally used to

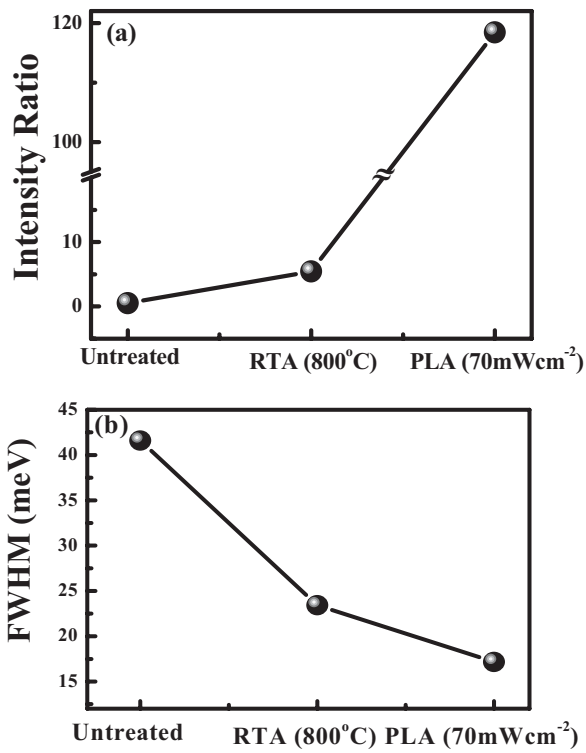

Figure 5 (a) The intensity ratios of PL for the RTA(800 °C)- and PLA(70 mJ/cm^2)-treated to untreated ZnO nanorods. (b) The FWHM of PL for the RTA(800 °C)- and PLA(70 mJ/cm^2)-treated to untreated ZnO nanorods. The lines are guides for the eye.

characterize the quality of the ZnO nanorods. The larger intensity ratio reveals that the ZnO nanorods have better crystallization or fewer defects. We find that the intensity ratio of the ZnO nanorods with PLA is larger than that with RTA, as displayed in Fig. 5a. This indicates that the ZnO nanorods treated with PLA have better crystalline quality (fewer defects) than that with RTA. The full width at half-maximum (FWHM) of UV exciton emission can also be used to characterize the quality of ZnO nanorods. Figure 5b shows the FWHM of UV exciton emission extracted from Fig. 5. The FWHM decreases from 42 to 17 (23) cm^{-1} with PLA (RTA) treatment, in good agreement with the result of the PL intensity ratio also. Therefore, we suggest that the treatment of PLA is more advantages than that of RTA for ZnO nanorods because PLA produces better crystalline quality, and it can be carried out in air. The improvement of luminescence properties may make the ZnO nanorods particularly useful for the further applications in optoelectronics.

To investigate surface morphology of ZnO nanorods after PLA, ZnO nanorods were examined with scanning electron microscopy (SEM). Figure 6a shows the untreated ZnO nanorods grown on Si substrate. Figure 6b–f shows the ZnO nanorods after PLA at fluences of 10, 30, 40, 50, and 70 mJ/cm^2, respectively. After annealing with a fluence of 30 mJ/cm^2 (Fig. 6c), the ZnO nanorods start to melt and their surface morphology changes. At the higher fluences of 40–70 mJ/cm^2 (Fig. 6d–f), ZnO nanorods are largely destroyed and merge into pieces. It is noted that the pronounced morphology change of ZnO nanorods with PLA at fluences of 30 and 40 mJ/cm^2 (Fig. 6c and d) corresponds to the decrease of PL intensity (Fig. 2b). Further deterioration of morphology in nanorods due to higher fluences does not lead to a reduction of the PL intensity; on the contrary, it leads to the enhancement of PL intensity. The PL intensity of ZnO nanorods is thus not associated with the surface morphology only. In other words, another mechanism also leads to a change of PL intensity after PLA.

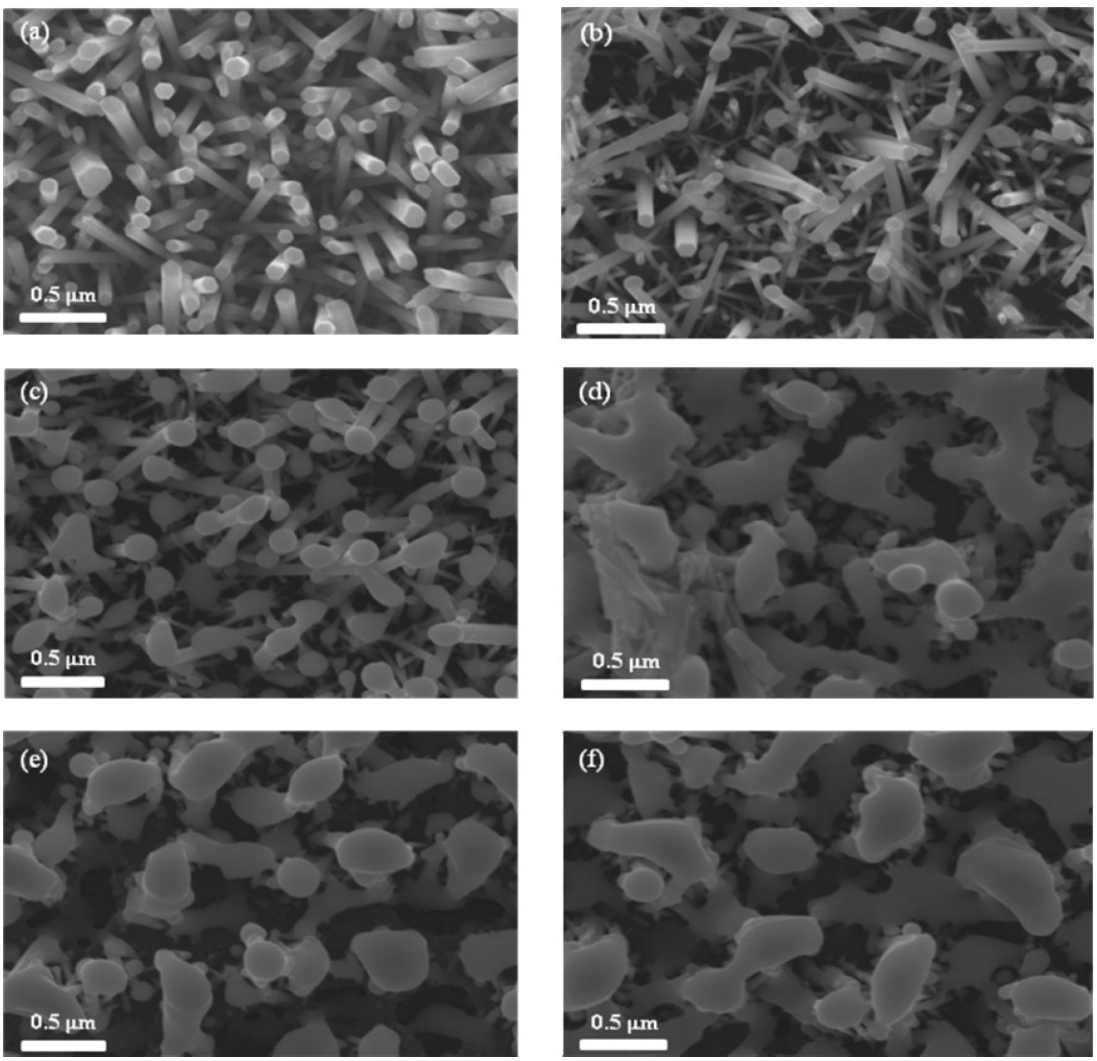

Figure 6 (a) SEM micrograph of the untreated ZnO nanorods, (b)–(f) SEM micrographs of the ZnO nanorods annealed by PLA with fluence at 10, 30, 40, 50, and 70 mJ/cm^2, respectively.

Aoki et al. [18] reported that on using the KrF excimer laser irradiation in the PLA the intensity of the UV emission decreases owing to deterioration of the surface crystallinity of single crystal ZnO wafers. On the other hand, Zhao and Jiang [19] observed an increase of UV emission after the PLA in ZnO films. They proposed that the mechanism responsible for the UV enhancement is the increase in the donor density and not the improvement in the crystalline quality. In our case, we suggest that the change of UV PL in the ZnO nanorods after PLA is not dependent on the surface morphology only, but also related to the dopant density. During PLA the photon energy of pulsed laser is sufficient to break Zn–O bonds, producing the point defects oxygen vacancies (V_O) and/or zinc interstitials (Zn_i), which act as n-type dopants [19]. Therefore, the donor density in ZnO nanorods increases after PLA, as shown in Fig. 2b. However, PLA at a fluence of about 30 mJ/cm^2 may cause deterioration in the morphology of ZnO nanorods. This effect leads to a decrease of PL intensity at a range of fluencies from 20 to 40 mJ/cm^2. After the fluence of 40 mJ/cm^2, deterioration in the morphology is not pronounced (Fig. 6d–f), leading the PL intensities to keep increasing with fluence due to the increase of dopant densities. Thus, the PL data as a function of fluence can be well explained by a combination of the deterioration of surface morphology in nanorods and the increase of dopant density due to the irradiation of pulsed lasers.

In order to understand whether the oxygen vacancy plays a role in the PL of ZnO nanorods, the PLA under various oxygen partial pressures were performed. Figure 7 shows the PL spectra of ZnO nanorods with PLA under several oxygen pressures. It was found that the PL intensity with the PLA treatment in an oxygen atmosphere decreases as the oxygen pressure is increased. The PL intensity as a function of the oxygen pressure is displayed by Fig. 8. The PL intensity decreases pronouncedly in the low-pressure range (0.02–40 Torr), then slowly in the range of 40–750 Torr. We suggest that the oxygen vacancies can be passivated (occupied) by the oxygen, leading to the decrease of oxygen vacancies and hence the decrease of the dopant density. The PL intensity

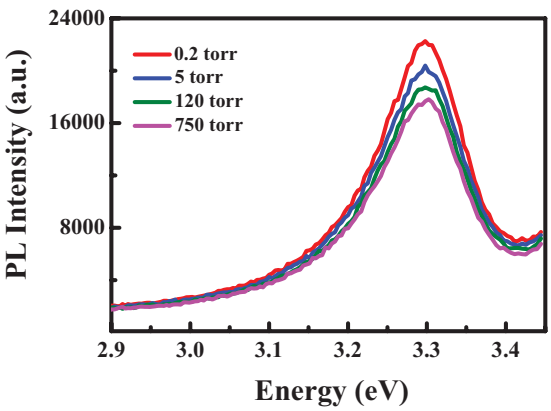

Figure 7 (online color at: www.pss-a.com) PL spectra of the ZnO nanorods with PLA under different oxygen pressures.

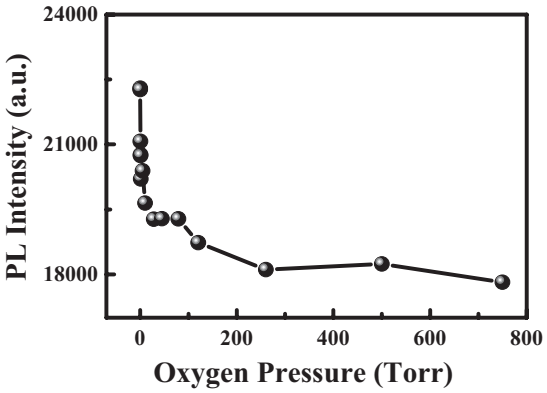

Figure 8 The PL intensity of the ZnO nanorods with PLA versus the oxygen pressure. The line is a guide for the eye.

quenches accordingly since the dopant density gives rise to the PL in the ZnO nanorods. In the low-pressure range (0.02–40 Torr), the oxygen vacancies can be occupied by oxygen easily and thus the numbers of the oxygen vacancies decreases rapidly, leading to a pronounced decrease of the PL intensity. In the high-pressure range, most of the sites of the oxygen vacancies may have been occupied, hence the decrease of the oxygen vacancies becomes slow. This explains the slow decrease of the PL intensity as a function of the oxygen pressure. According to this observation, we are inclined to suggest that the oxygen vacancies act as n-type dopants and contribute to the luminescence in ZnO nanorods.

4 Summary In summary, the effect of PLA and RTA on the luminescence characteristics of ZnO nanorods was studied. The UV PL in ZnO nanorods shows a general increasing trend as the fluence of pulsed lasers increases, except at a range of fluencies from 20 to 40 mJ/cm^2. It is found that the treatment with the PLA at the fluence of 70 mJ/cm^2 produces a larger improvement of crystalline in ZnO nanorods, comparing to the treatment with RTA. A combination of the increase in donors and the deterioration in the surface crystallinity of the ZnO nanorods is suggested to be responsible for the intensity change of UV PL after PLA. We also find that the PL of ZnO nanorods can be affected by an oxygen atomosphere, and oxygen vacancies play a role in the PL of ZnO nanorods.

Acknowledgements This project was supported in part by the National Science Council under the grant numbers NSC 100-2112-M-033-005-MY3 and NSC 100-2627-M-033-002 and by the Institute of Nuclear Energy Research under the grant number 1002001INER042.

References

[1] T. Shibata, K. Unno, E. Makino, Y. Ito, and S. Shimad, Sens. Actuators A **102**, 106–113 (2002).
[2] Y. L. Wang, H. S. Kim, D. P. Norton, S. J. Pearton, and F. Ren, Appl. Phys. Lett. **92**, 112101 (2008).

[3] M. Purica, E. Budianu, and E. Ruso, Microelectron. Eng. **51/52**, 425–431 (2000).
[4] M. Suchea, S. Christoulakis, K. Moschovis, N. Katsarakis, and G. Kiriakidis, Thin Solid Films **515**, 551–554 (2006).
[5] Z. K. Tang, G. K. L. Wong, P. Yu, M. Kawasaki, A. Ohtomo, H. Koinuma, and Y. Segawa, Appl. Phys. Lett. **72**, 3270–3272 (1998).
[6] D. C. Reynolds, D. C. Look, B. Jogai, C. W. Litton, G. Cantwell, and W. C. Harsch, Phys. Rev. B **60**, 2340–2344 (1999).
[7] S. Y. Myong, K. Sriprapha, S. Miyajima, M. Konagai, and A. Yamada, Appl. Phys. Lett. **90**, 263509 (2007).
[8] J. Grabowska, A. Meaney, K. K. Nanda, J.-P. Mosnier, M. O. Henry, J.-R. Duclére, and E. McGlynn, Phys. Rev. B **71**, 115439 (2005).
[9] C. C. Lin, H. P. Chen, H. C. Liao, and S. Y. Chen, Appl. Phys. Lett. **86**, 183103 (2005).
[10] C. Liu, Y. Masuda, Y. Wu, and O. Takai, Thin Solid Films **503**, 110–114 (2006).
[11] A. Nadarajah and R. Könenkamp, Nanotechnology **22**, 025205 (2011).
[12] S. Wei, J. Lian, and H. Wu, Mater. Charact. **61**, 1239–1244 (2010).
[13] L. H. Quang, S. J. Chua, L. K. Ping, and E. Fitzgerald, J. Cryst. Growth **287**, 157–161 (2006).
[14] L. L. Yang, Q. X. Zhao, M. Willander, and I. Ivanov, J. Appl. Phys. **105**, 053503 (2009).
[15] J. Qiu, J. W. Kim, I. J. Lee, B. Kim, H.-K. Kim, and Y.-H. Hwang, Phys. Status Solidi A **208**, 1021–1026 (2011).
[16] S. Shi, J. Xu, X. Zhang, and L. Li, J. Appl. Phys. **109**, 103508 (2011).
[17] M. Z. Sahdan, S. Amizam, H. A. Rafaie, Z. Khusaimi, A. Z. Ahmed, S. Abdullah, and M. Rusop, in: IEEE Int. Conf. on Semiconductor Electronics, Johor Bahru, Malaysia, 2008, pp. 566–570.
[18] T. Aoki, Y. Hatanaka, and D. C. Look, Appl. Phys. Lett. **76**, 3257–3259 (2000).
[19] Y. Zhao and Y. Jiang, J. Appl. Phys. **103**, 114903 (2008).
[20] C. Boemare, T. Monteiro, M. J. Soares, J. G. Guilherme, and E. Alves, Physica B **308–310**, 985–988 (2001).

